Arch Environ Contam Toxicol
DOI 10.1007/s00244-013-9975-4

Pulmonary Inflammation and Cell Death in Mice After Acute Exposure to Air Particulate Matter From an Industrial Region of Buenos Aires

F. Astort · M. Sittner · S. A. Ferraro · N. S. Orona · G. A. Maglione · A. De la Hoz · D. R. Tasat

Received: 6 September 2013 / Accepted: 18 November 2013

Abstract Epidemiological studies have shown that air particulate matter (PM) can increase respiratory morbidity and mortality being the lungs the main target organ to PM body entrance. Even more, several *in vivo* and *in vitro* studies have shown that air PM has a wide toxicity spectra depending among other parameters, on its size, morphology, and chemical composition. The Reconquista River is the second most polluted river from Buenos Aires, and people living around its basin are constantly exposed to its contaminated water, soil and air. However, the air PM from the Reconquista River (RR-PMa) has not been characterized, and its biological impact on lung has yet not been assessed. Therefore, the present investigation was undertaken to study (1) RR-PMa morphochemical characteristic and (2) RR-PMa lung acute effects after intranasal instillation exposure through the analysis of three end points: oxidative stress, inflammation, and apoptosis. A single acute exposure of RR-PMa (1 mg/kg body weight) after 24 h caused significant ($p < 0.05$) enrichment in bronchoalveolar total cell number and polymorphonuclear (PNM) fraction, superoxide anion generation, production of pro-inflammatory cytokines TNF-α and IL-6, and induction of apoptosis. It was also observed that in lung homogenates, none of the antioxidant enzymes assayed showed differences between exposed RR-PMa and control mice. These data demonstrate that air PM from the Reconquista River induce lung oxidative stress, inflammation, and cell death therefore represents a potential hazard to human health.

Air pollution results from a complex mixture of gases and particles. Its composition varies with the occurrence of diverse gases concentrations and particles from suspended soil components, biological sources, and combustion-derived components from industrial and engine technologies (Forastiere et al. 2005). Every day exposure to airborne particulate matter (PM) pollution in urban areas is associated with increased morbidity and mortality mainly due to cardiorespiratory diseases (Krewski et al. 2000; Pope et al. 2009; Saldiva 1998; Beelen et al. 2009).

Epidemiologic findings indicate that the greatest health risks correlate with smaller particles, which have the ability to reach deeper into the lungs (Oberdorster 2001). However, PM biologic effects seem to vary among different urban areas, which could partially be explained due to its different emission sources and composition (Schins 2002; Perrone et al. 2013). In particular, components such as transition metals and polycyclic aromatic hydrocarbons, either through adherence to the core particle or as an integral component of the particle, are known to be associated with PM unfavorable health effects (Dreher et al. 1997; Dye et al. 2001; Nel et al. 2001). Proposed mechanisms behind PM-induced health effects are oxidative stress (Nel et al. 2001; Tao et al. 2003) and inflammation associated injury (Dick et al. 2003; Ghio and Devlin 2001).

F. Astort (✉) · M. Sittner · S. A. Ferraro · N. S. Orona · G. A. Maglione · A. De la Hoz · D. R. Tasat
School of Science and Technology, National University of General San Martín, Martín de Irigoyen 3100 (1653), San Martín, Buenos Aires, Argentina
e-mail: pacoastort@gmail.com

S. A. Ferraro · N. S. Orona
Committee for Scientific Research, Calle 526 entre 10 y 11 (1900), La Plata, Buenos Aires, Argentina

D. R. Tasat
School of Dentistry, University of Buenos Aires, MT de Alvear 2142, (C1122AAH), Buenos Aires, Argentina

Published online: 11 December 2013

The Reconquista River (RR), one of the most polluted watercourses in Argentina, receives effluent discharges from heavily industrialized and highly populated settlements. During winter and summer time, the floodplain remains dry, producing the oxidation of sulfide and organic matter present in the soil, thus making heavy metals more bioaccessible. Dispersion of soil particles occurs, and thus harmful effects on the pulmonary health of residents and workers inhabiting the RR bank may take place.

In this context, we recently analyzed the composition and biological impact of the PM from RR sediment (RR-PMs) on lung mice (Ferraro et al. 2012). We showed that RR-PMs composition includes particles of heterogeneous sizes (agglomerates PM10 and PM2.5) with the presence, in its bioaccesible phase, of metals traces such as lead (Pb), cadmium (Cd), chromium (Cr) and sulfur (S) and that the cytotoxic and proinflammatory effects found in the respiratory tract are mostly determined by its metal content.

Since a direct correlation between the impact on health induced by RR-PMs plausible to get suspended and because air particles from the same area may not be consistent, the purpose of the present study was to (1) collect and morphochemically characterize airborne PM from the Reconquista River (RR-PMa); and (2) determine whether RR-PMa compromises pulmonary function due to an imbalance in the oxidative metabolism. To elucidate RR-PMa's biological impact, we acutely instilled RR-PMa into mice lungs and studied the production of free radicals and antioxidant enzymes either in bronchoalveolar lavage fluid (BALF) cells or in lung homogenates. Furthermore, we evaluated the proinflammatory production and cell death in BALF cells from control and exposed mice as possible targets of oxidative metabolism imbalance.

Materials and Methods

Drugs and Chemicals

Nitroblue tetrazolium (NBT), 12-*O*-tetradecanoylphorbol 13-acetate (TPA), ethylenediaminetetraacetic acid, phosphate buffer saline (PBS), polyvinylpyrrolidone, paraformaldehyde, bovine albumin, and all histological dyes employed were purchased from Sigma-Aldrich (MI, USA). Purified monoclonal antibodies for interleukin 6 (IL-6) and tumor-necrosis factor (TNF-α) were purchased from BD Pharmingen (CA, USA).

Site Description and Air Sampling

Samples were collected in "La Carcova," a poor neighborhood located on the north side of the Buenos Aires city (location-34.521205, -58.584042) by the RR during summer time (temperature 25.2 °C, humidity 64 %, wind 5 km/h, wind direction northeast, pressure 1011.7 h Pa, rainfall 41.6 mm [total]). The inhabitants of this neighborhood are subject to PM air pollution arising from (1) motor vehicle emission from the nearby highway, (2) heavily contaminated dry RR floodplain, (3) bordering dumpsites, and (4) nearby activity of a clay industry located at a distance <2000 m (Fig. 1, GoogleMaps).

A MiniVol Portable Air Sampler (Airmetrics, OR, USA) with 2.5-μm cut-point impactors using a flow rate of 5 L min^{-1} was employed (Baldauf et al. 2001). The samples were collected on Teflon filters (37 mm, Pleion, 0.8-μm pore size), and each filter was placed in a clean plastic cassette during transport and storage. The filters were weighed (after moisture equilibration) before and after sampling to determine the net particulate mass gain with a microbalance (Mettler M3, weighing accuracy of 1 μg), using α source to remove the electrostatic charge.

Particle Characterization

Scanning electron microscopy (SEM) and energy dispersive X-ray spectroscopy (EDX) were employed to analyze particle morphology and chemical composition. For SEM observations, collected particles were coated with gold by direct current sputtering. Stub preparations were examined in a quanta SEM FEG-S50 (FEI, OR, USA). Chemical composition was analyzed with a Phillips SEM 505 (FEI, OR, USA) coupled to a EDX dispersion detection unit (EDAX Inc., NJ, USA).

Animal Exposure to Air Particle Matter From RR-PMa

Young male BALB/c mice (1–2 months old) were obtained from the animal facilities of the School of Exact and Natural Sciences, University of Buenos Aires. Animals were housed and fed a normal protein diet *ad libitum* at the breeding facility of the School of Science and Technology, University of San Martín, for use throughout these experiments. Housing was performed according to the Care and Use of Laboratory Animals from the National Institutes of Health Guide. All experiments act in accordance with local ethical guidelines (Ethical Committee from the National University of General San Martín).

BALB/c mice were exposed to RR-PMa by intranasal instillation. This technique is effective and noninvasive and is commonly used in toxicity studies (Leong et al. 1998) where the distribution pattern of particles is of crucial importance. Briefly, this instillation technique consists in deliver drop-wise the particle suspension or the vehicle to the nares, using a micropipette, while the mouse is in a supine position (Southam et al. 2002). Animals were lightly anesthetized intraperitoneally with 1 ml/kg bw of

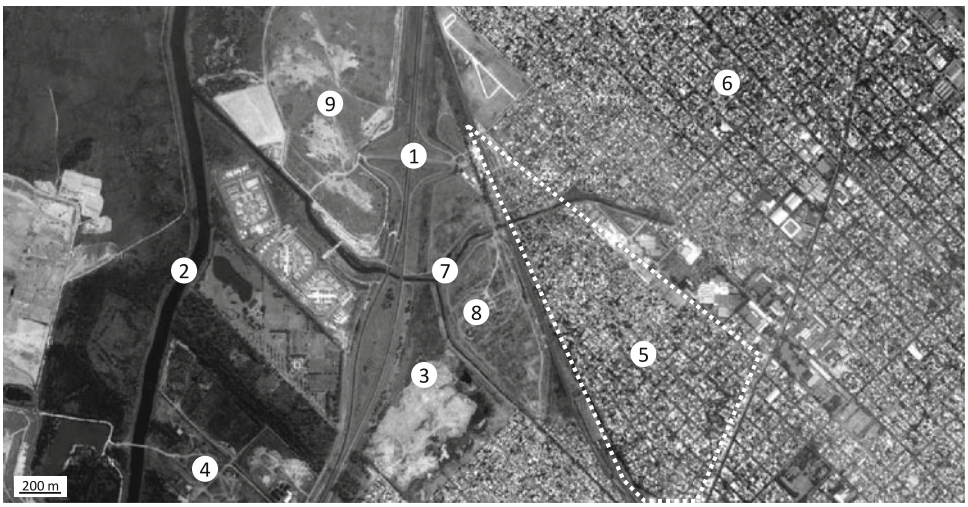

Fig. 1 Satellite photograph of La Carcova neighborhood and surroundings. *1* highway Camino del Buen Aire, *2* RR, *3* active landfill, *4* clay industry, *5* sample site, *6* residential zone, *7* RR's streams, *8* and *9* landfill. The *white dotted line* represents the boundaries of La Carcova

xylazine (2 %) and ketamine (50 mg/ml) and intranasally instilled with 50 µl of free-particle PBS (control group) or 1 mg/kg bw RR-PMa suspended in the same vehicle (exposed animals). For the acute exposure, particles from the RR were suspended in sterile PBS and sonicated during 10 min before use.

Animals were killed 24 h after intranasal instillation with an overdose of xylazine–ketamine. The selection of the RR-PMa dose was based on previous studies where acute PM effect was analyzed (Ferraro et al. 2011; Magnani et al. 2011; Gurgueira et al. 2002; Ghio et al. 2002; Nurkiewicz et al. 2006; Marchini et al. 2013).

From all control and exposed RR-PMa animals, BALF fluid was obtained and the following end points evaluated: total cell number (TCN), cell differential, superoxide anion production, proinflammatory cytokines, and apoptosis. Antioxidant enzyme analysis was performed in lung tissue homogenates (Fig. 2).

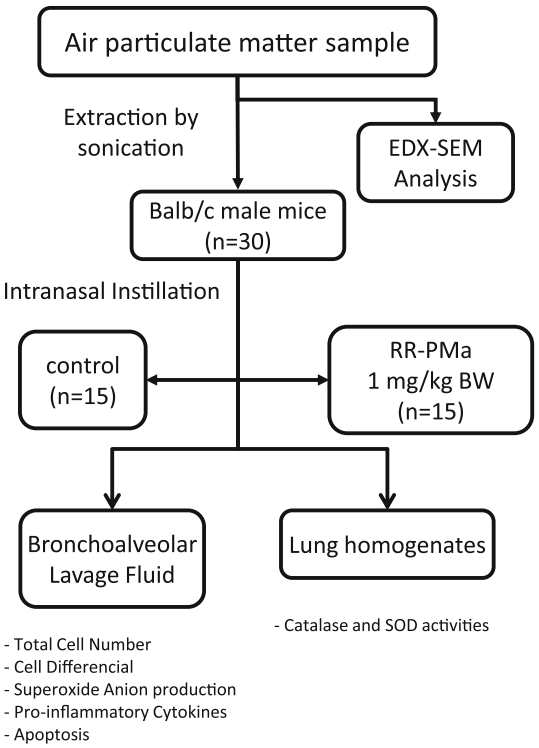

Fig. 2 Experimental protocol diagram. Animals were randomized into two groups and exposed to intranasal instillation with PBS (*control*) or exposed to RR-PMa particle (*1 mg/kg bw*). All biological parameters were determined 24 h after animal exposure

Broncho Alveolar Lavage Fluid (BALF)

BALF was obtained as previously described by our group (Tasat and de Rey 1987). Briefly, the thoracic cavity was partly dissected and the trachea cannulated with an 18-gauge needle. The excised lung was then gently massaged and lavaged 12 times with 1 ml of cold sterile PBS. BALF was immediately centrifuged at 800×*g* for 10 min at 4 °C, and TCN was determined using a Neubauer chamber.

Total Cell Number (TCN) and Differential Cell Count (DCC)

Bronchoalveolar lavage TCN was determined with a Neubauer chamber. DCC was determined after cell fixation with methanol and staining with hematoxylin–eosin. At least 200 cells in each sample were counted by light microscopy (Ferraro et al. 2012).

Superoxide Anion Generation

Superoxide anion (O_2^-), a main reactive oxygen species generated during the respiratory burst, was evaluated using the NBT test (Segal 1974). BALF cells were treated with

NBT in the presence or absence of 12-*O*-TPA, a known inductor of O_2^- production. All tubes were incubated with NBT for 45 min at 37 °C. O_2^- intracellular production is evidenced by the amount of a blue formazan precipitate in the cells after NBT reduction. Cells were scored by light microscopy as described elsewhere (Molinari et al. 2000).

Tissue Homogenates and Protein Determination

Lung samples (0.2 g wet weight) from control and exposed BALB/c mice were homogenized in PBS at 0–4 °C. The suspension was centrifuged at 600×*g* for 10 min at 4 °C to remove cell debris (Evelson and Gonzalez-Flecha 2000). The pellet was discarded and the supernatant used for antioxidant activity determinations. Protein was measured by the method of Lowry et al. (1951) using bovine serum albumin as the standard.

Superoxide Dismutase (SOD) and Catalase (CAT) Activities

SOD activity was determined spectrophotometrically by measuring the inhibition rate of the autocatalized formation of adenochrome at 480 nm in a reaction medium containing 1 mM of epinephrine and 50 mM of glycine/NaOH (pH 10.5) (Misra and Fridovich 1972). Enzymatic activity was expressed as units (U) per milligram of protein. One U is defined as the amount of enzyme that inhibits the rate of adrenochrome formation by 50 %. CAT activity was determined by measuring the decrease in absorption at 240 nm in a reaction medium consisting of PBS and 20 mM of hydrogen peroxide (Maehly and Chance 1954). Results were expressed as arbitrary units (AU) of CAT activity per milligram of protein.

Proinflammatory Cytokine Production

Production of proinflammatory cytokines was evaluated in BALF of control and RR-PMa-exposed animals. Tumor necrosis factor alpha (TNF-α) and interleukin 6 (IL-6) were evaluated on the first milliliter of BALF. Supernatants were kept frozen at −20 °C until use. Both cytokines were detected using a specific enzyme-linked immunosorbent assay (ELISA). Briefly, ELISA plates (Corning, Newark, California) were coated with 1:125 TNF-α or 1:83 IL-6 specific capture antibody diluted in coating buffer (0.1 M of sodium carbonate [pH 6] for TNF-α or 0.1 M of sodium phosphate [pH 9.5] for IL-6) at 4 °C overnight. Wells were washed (0.05 % Tween 20) and blocked with PBS containing 10 % fetal bovine serum for 2 h at room temperature (RT). Cytokine standards and samples were added to wells in triplicate and incubated at 4 °C overnight. After three washes, biotinylated cytokine-specific detection antibodies 1:250 were added for 1 h. After washing, the detection agent streptavidin–peroxidase was used with the substrate tetramethylbenzidine for 30 min. Absorbance was measured at 655 nm on a microplate reader (Benchmark; BioRad, CA, USA).

Morphological and Immunocytochemical Evaluation of Apoptosis

Morphological evaluation of apoptosis was performed in BALF cells of control and RR-PMa-exposed mice. Cells were washed twice with PBS, fixed in acetic-methanol (1:3) for 10 min, and stained with 5 μg/ml of Hoechst 33258 in PBS for 15 min. Morphological features, such as pyknosis and nuclear fragmentation (Singhal et al. 1998), were examined under 460 nm in a fluorescent light microscope (Axioskop Microscope; Carl Zeiss, Oberkochen, Germany).

Immunocytochemical determination of apoptosis was performed by the detection of active caspase-3 and cleavage of poly ADP-ribose polymerase (PARP). Control and exposed BALF cells were fixed in 4 % paraformaldehyde for 20 min at RT and permeabilized with 0.2 % Triton X-100 for 7 min. Subsequently, cells were blocked with blocking buffer (PBS 0.1 %, Tween 20, and 5 % normal serum) in a moist chamber for 2 h. Then cells were incubated with primary antibody against either active caspase-3 (1:500) or 85-kDa PARP cleavage fragment (1:250) for 2 h. Then all wells were washed twice with PBS and twice with PBS/0.1 % Tween 20. To localize the expression of these apoptotic markers, cell smears were incubated with a secondary antibody conjugated to Cy3 (1:250) for 60 min and the reaction visualized under a fluorescent light microscope (Axioskop Microscope; Carl Zeiss, Oberkochen, Germany).

Statistical Analysis

The results corresponding to the end points for control and exposed animals were compared by Student *t* test or one-way analysis of variance (ANOVA) with Tukey's multiple comparisons post test. Statistical significance was set at $p < 0.05$. The number of animals and experiments for each group (control and exposed) are shown in the legends of each figure.

Results

Morphological and Chemical Analysis of RR-PMa

RR-PMa morphology was analyzed by SEM. As shown in Fig. 3AI, RR-PMa ranged from 0.1 μm (ultrafine) to 10 μm

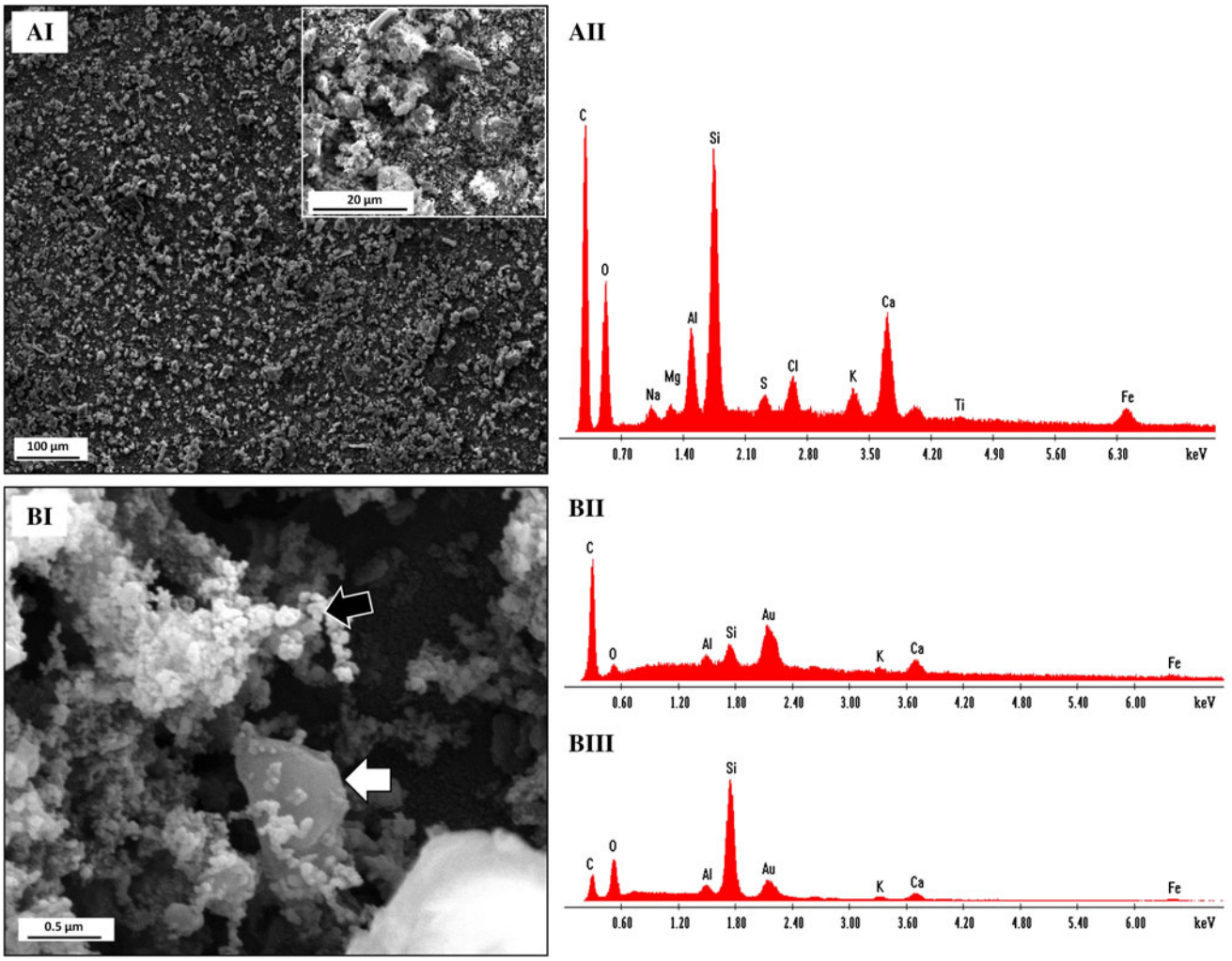

Fig. 3 Morphological and chemical analysis of RR-PMa. **AI** SEM microphotograph of RR-PMa shows particle heterogeneous morphology. Magnification = ×150, scale = 100 µm. *Inset* magnification = ×5000, scale = 20 µm. **AII** EDX analysis of the whole sample including all particle sizes. EDX shows the characteristic elemental chemical composition (intensity in function of energy in KeV). **BI** SEM microphotograph of RR-PMa shows ultrafine particles (*black arrow*) and fine particles (*white arrow*) ranging from <1 µm and 1–10 µm aerodynamic diameter size, respectively. Magnification = ×80,000, scale = 0.5 µm. EDX from **BII** ultrafine, and **BIII** fine particles

(fine) particle size. Chemical composition analysis by EDX showed the presence of a carbonaceous core containing traces of aluminum silicates, magnesium, potassium, iron, calcium, chlorine, titanium, and sulfur (Fig. 3AII).

Based on their size and shape, mainly two very different particle populations can be described: (1) small spherical ultrafine particles (<0.1 µm) free or grouped in agglomerates resembling bunches of grapes (Fig. 3BI, black arrow); or (2) larger nonspherical particles (<10 µm) (Fig. 3BI, white arrow). EDX analysis showed that ultrafine particles are composed mainly by the carbon element (Fig. 3BII), whereas larger particles presented mostly aluminum silicates, ions, and trace metals (Fig. 3BIII).

BALF Analysis from Control and RR-PMa-Exposed Mice

As shown in Fig. 4A, RR-PMa intranasal instillation induced a significant increase in TCN compared with controls. Then we evaluated the contribution of different cell populations in BALF by quantifying the percentage of alveolar macrophages (AM), polymorphonuclear cells (PMN), and lymphocytes (L).

BALF obtained from control nonexposed animals elicited a normal cell population distribution characterized by 86.0 ± 1.1 % of AM and 11.7 ± 0.8 % of PMN. In contrast, as shown in Fig. 4B, instillation of RR-PMa provoked

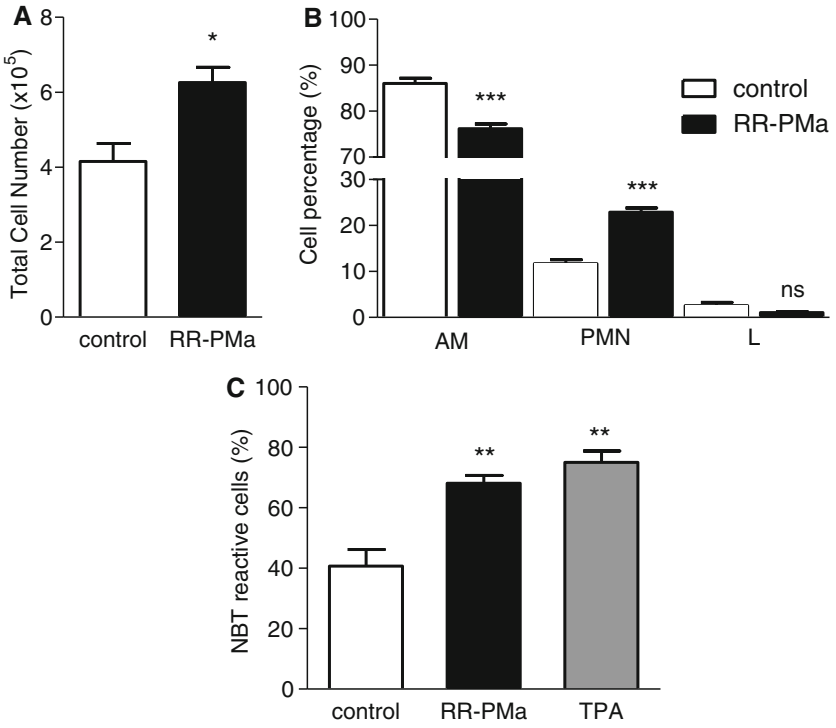

Fig. 4 BALF analysis from control and RR-PMa-exposed mice. **A** TCN, and **B** DCC. Data are mean ± SEM, $n = 15$/group, $*p < 0.05$, $***p < 0.001$ (Student t test). **C** Generation of O_2^- in BALF cells determined by quantitative reduction of NBT. Data are mean ± SEM, $n = 7$/group, $**p < 0.01$, ANOVA (Tukey's multiple comparison test)

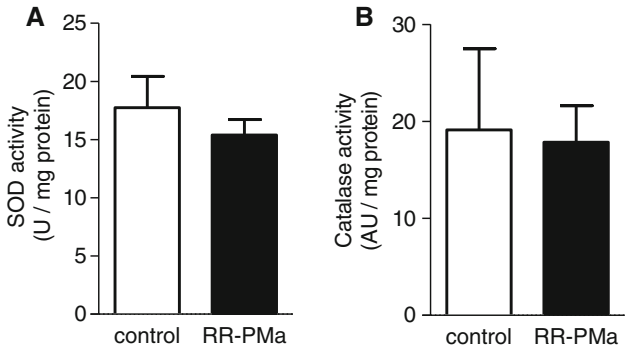

Fig. 5 Effect of RR-PMa on antioxidant defense in mice lung homogenates. **A** SOD, and **B** CAT activities assayed in lung homogenates from control and RR-PMa-exposed mice. No significant differences were observed between these two groups. Data are mean ± SEM, $n = 5$/group, $p > 0.05$ (Student t test)

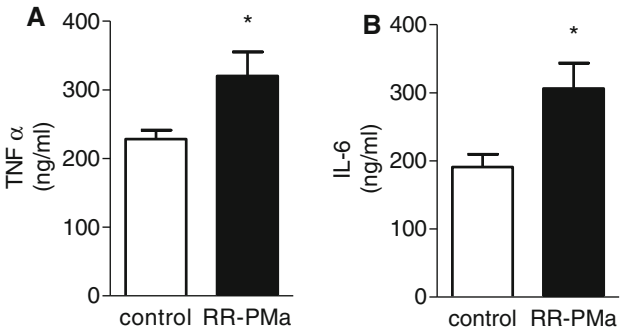

Fig. 6 Effect of RR-PMa on BALF proinflammatory cytokine levels. BALF from control and RR-PMa-exposed mice were obtained 24 h after instillation and assessed either for **A** TNF-α or **B** IL-6. Both proinflammatory cytokines were measured by ELISA. Data are mean ± SEM, $n = 8$, $*p < 0.05$ (Student t test)

a significant increase in PMN percentage (RR-PMa = 22.8 ± 3.9 % vs. control = 11.7 ± 3.4 %; $n = 15$, $p < 0.001$, Student t test). It is worth to note that the percentage of L always remained <3 % irrespective of treatment.

Superoxide Anion Generation

RR-PMa exposure induced a significant increase of the percentage of reactive BALF cells compared with controls (RR-PMa = 68.2 ± 2.5 % vs. control = 40.7 ± 5.6 %; $n = 6$, $p < 0.001$, Student t test). RR-PMa and TPA, employed as a positive control, induced superoxide anion generation reaching almost similar reactive cell percentages (Fig. 4C).

Antioxidant Enzymes Activities in Mouse Lung Homogenates

SOD are a group of antioxidant enzymes that catalyze the dismutation of superoxide anion to oxygen and hydrogen peroxide, whereas CAT is the main detoxifying system for hydrogen peroxide.

As shown in Fig. 5, neither SOD nor CAT activities assayed in lung homogenates showed significant differences between RR-PMa and control mice (SOD:

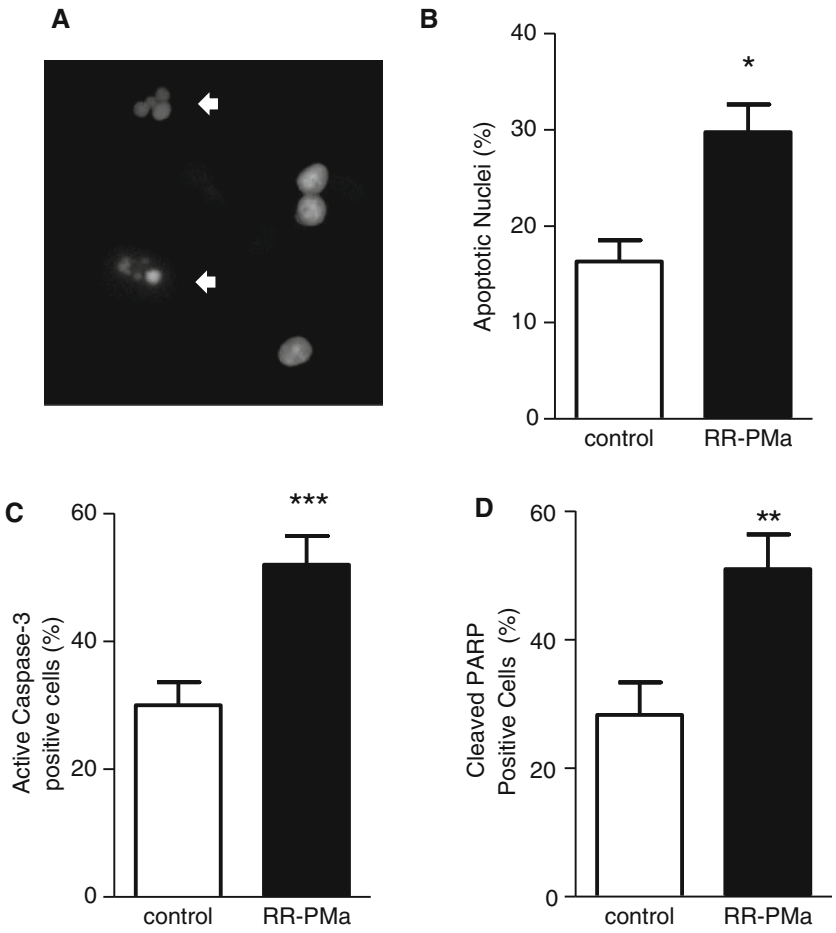

Fig. 7 Effect of RR-PMa on BALF cell apoptosis. **A** Representative microphotograph from RR-PMa BALF showing nuclear staining by Hoechst 33342. *Arrows* indicate apoptotic condensed nuclei. Magnification ×1000. **B** Quantification of percentage (%) of cells in apoptotic process in both control and RR-PMa-exposed BALF. Data are mean ± SEM, $n = 5$, $^{*}p < 0.05$ (Student t test). **C** and **D** Immunohistochemical analysis of active caspase-3 and cleaved PARP. **C** Quantification of percentage (%) of active caspase-3-positive cells. Data are mean ± SEM, $n = 14$, $^{***}p < 0.001$ (Student t test). **D** Quantification of percentage (%) of cleaved PARP-positive cells. Data are mean ± SEM, $n = 7$, $^{**}p < 0.01$ (Student t test)

control = 17.7 ± 5.3 vs. RR-PMa 15.4 ± 2.9 U/mg prot and CAT: control = 19.1 ± 8.3 vs. RR-PMa = 17.8 ± 3.7 AU/mg protein, n = 5, $p > 0.05$, Student t test).

Proinflammatory Cytokine Levels

As seen in Fig. 6, the two pro-inflammatory cytokines, TNF-α and IL-6, were significantly greater in BALF supernatant from RR-PMa-exposed mice compared with control animals (TNF-α control = 228 ± 12 vs. RR-PMa 320 ± 34 ng/ml; IL-6 control = 191 ± 18 *vs* RR-PMa 306 ± 37 ng/ml; $p < 0.05$, Student t test).

Morphological and Immunocytochemical Evaluation of Apoptosis

Morphological analysis using nuclear fluorescent Hoechst 33258 stain showed that RR-PMa induced a significant increase in the percentage of apoptotic cells in BALF. A representative microphotograph with normal cells eliciting homogeneous chromatin nuclei and apoptotic cells featuring condensed chromatin (arrows) are shown in Fig. 7A. Quantification of the apoptotic process in both control and exposed RR-PMa mice (control = 16.3 ± 2.2 % vs. RR-PMa 29.7 ± 2.9 %, $n = 5$, $p < 0.05$, Student t test) is shown in Fig. 7B.

The evaluation of two biological markers of apoptosis, active caspase-3 and cleaved PARP, is shown in Fig. 7C, D. The immunocytochemical study showed that RR-PMa was able to induce an increase in both active caspase-3 (control = 30 ± 4 % vs. RR-PMa = 52 ± 5 %; $p < 0.001$, Student t test) and cleaved PARP positive cells (control = 28 ± 5 % vs. RR-PMa = 51 ± 5 %; $p < 0.01$, Student t test).

Discussion

In this work we analyzed the physicochemical composition and biological effect of air PM from a semiurban location called La Carcova in the north outside area of Buenos Aires City (RR-PMa). To our knowledge, this is the first attempt to characterize and analyze RR-PMa morphochemical composition and biological effect. Our results show that RR-PMa is composed of particles with heterogeneous sizes ranging from fine to ultrafine. Based on their chemical composition, ultrafine particles could arise from vehicle (a highway called "Camino del Buen Aire") and biomass

combustion (nearby landfills and industries [see clay industry location on the map]) as the main emission sources. It is noteworthy that particles emitted from diesel engines are typically in the size range of 0.1 μm (ultrafine) and can also carry carcinogenic compounds adsorbed on their surface, such as benzopyrenes (Li et al. 2000; Schins 2002; Perrone et al. 2013).

On the contrary, and in agreement with previous work published by our group (Ferraro et al. 2012), larger particles presenting metal traces on their composition could derive mainly from the dry RR basin soil. In this zone, wind causes particle suspension moving dust grains containing aluminosilicates (Al_2O_3 and SiO_2), major components of clay minerals, from the river basin into the populated area. Prolonged and unprotected exposure of inhabitants to RR-PMa can induce respiratory (silicosis, lung cancer, etc.) and eye [keratoconjunctivitis sicca ("dry eyes")] diseases (Araujo 2010; Torricelli et al. 2011; Andreau et al. 2012).

The TCN and CCD in BALF are well-established parameters to identify inflammation events in the respiratory tract. In control mice, BALF AM are abundant, whereas PMN cells are rare with PMN percentage being a sensitive marker of lung inflammation (Henderson 2005). Thus, to analyze the acute biological impact on the respiratory system, mice were intranasally instilled with RR-PMa and TCN and CCD assayed. In agreement with other studies (Mantecca et al. 2010) we found an increase in TCN and altered BALF cell composition.

Direct reactive oxygen species generation by air pollution particles is attributed to both size and composition (Osornio-Vargas et al. 2003; Miller et al. 2012; Oberdorster 2001). It is well known that the smaller the particle (greater surface-to-volume ratio), the more toxic its effect (Araujo 2010; Ristovski et al. 2012). In particular, inhaled small particles can not only reach and accumulate in the lung alveoli triggering macrophages and PMNs superoxide anion generation in the lung, but they can cross cell membranes, spread into the bloodstream, and deposit in distant organs, thus increasing their persistence and harmfulness.

Regarding particle chemical composition, although it is believed that metals alter electron transport and also decrease levels of antioxidants, organic compounds act through redox cycling of quinone-based radicals and antioxidant depletion by reactions between quinones and thiol-containing compounds.

In our study, the superoxide anion increase observed in RR-PMa-exposed mice could be an adaptive response to both its small size and its composition (metallic traces in the fine and volatile organic compounds in the ultrafine particles).

Furthermore, RR-PMa induced secretion of TNF-α and IL-6, two pro-inflammatory cytokines. These results are consistent with previous observations where particles from different sources trigger pulmonary inflammation (Rosas Perez et al. 2007; Dick et al. 2003). Considering the complexity of PM composition related to multiple sources, it is not easy to speculate which components are responsible for activating the molecular mechanisms able to induce TNF-α and IL-6 secretion. The use of specific inhibitors of PM components or PM fractions might shed light on this matter.

The increase in proinflammatory cytokines and the nonresponse of defense antioxidants enzymes may commit the cell to an altered and lasting oxidative state, which could lead to cell death (Donaldson et al. 2003; Chirino et al. 2010). In fact, we found that both the percentage of active caspase-3 and PARP-positive cells augmented in BALF from RR-PMa-exposed mice.

We believe that the release of superoxide anion in response to RR-PMa could be the key orchestrating mediator driving the tissue to an oxidative state, which in turn could initiate a series of cellular and tissue reactions, including the release of inflammatory cytokines, that ultimately may end in cell injury and/or apoptosis.

This study brings original evidence on the adverse effects elicited by acute air particle exposure, mainly from anthropogenic origin, on the respiratory tract where the concentration mimics those currently observed in megacities worldwide (Beijing, China, January 12, 2013 = 755 $\mu g/m^3$ and October 29, 2013 = 429 $\mu g/m^3$; New Delhi, India, January 24, 2013 = 402 $\mu g/m^3$; Anand Vihar, New Delhi, India, October 29, 2013 = 999 $\mu g/m^3$; and Stefanikova, Kosice, Slovakia, October 29, 2013 = 163 $\mu g/m^3$). Future additional studies are needed to elucidate the contribution of each emission source on the cytotoxicity induced by the air particles from the RR industrial area and the potential impact on the health of the suburban population.

Acknowledgments We especially thank Gisela Maxia for technical assistance with SEM and EDX and Paulo H. Saldiva for kindly providing the collector sampler. This study was supported by the Agencia de Promoción Científica y Técnica from Argentina (Grant No. PICT-2010-1660).

References

Andreau K, Leroux M, Bouharrour A (2012) Health and cellular impacts of air pollutants: from cytoprotection to cytotoxicity. Biochem Res Int 2012:493894

Araujo JA (2010) Particulate air pollution, systemic oxidative stress, inflammation, and atherosclerosis. Air Qual Atmos Health 4(1):79–93

Baldauf RW, Lane DD, Marote GA (2001) Ambient air quality monitoring network design for assessing human health impacts from exposures to airborne contaminants. Environ Monit Assess 66(1):63–76

Beelen R, Hoek G, Houthuijs D, van den Brandt PA, Goldbohm RA, Fischer P et al (2009) The joint association of air pollution and noise from road traffic with cardiovascular mortality in a cohort study. Occup Environ Med 66(4):243–250

Chirino YI, Sanchez-Perez Y, Osornio-Vargas AR, Morales-Barcenas R, Gutierrez-Ruiz MC, Segura-Garcia Y et al (2010) PM(10) impairs the antioxidant defense system and exacerbates oxidative stress driven cell death. Toxicol Lett 193(3):209–216

Dick CA, Singh P, Daniels M, Evansky P, Becker S, Gilmour MI (2003) Murine pulmonary inflammatory responses following instillation of size-fractionated ambient particulate matter. J Toxicol Environ Health A 66(23):2193–2207

Donaldson K, Stone V, Borm PJ, Jimenez LA, Gilmour PS, Schins RP et al (2003) Oxidative stress and calcium signaling in the adverse effects of environmental particles (PM10). Free Radic Biol Med 34(11):1369–1382

Dreher KL, Jaskot RH, Lehmann JR, Richards JH, McGee JK, Ghio AJ et al (1997) Soluble transition metals mediate residual oil fly ash induced acute lung injury. J Toxicol Environ Health 50(3):285–305

Dye JA, Lehmann JR, McGee JK, Winsett DW, Ledbetter AD, Everitt JI et al (2001) Acute pulmonary toxicity of particulate matter filter extracts in rats: Coherence with epidemiologic studies in Utah Valley residents. Environ Health Perspect 109(Suppl 3):395–403

Evelson P, Gonzalez-Flecha B (2000) Time course and quantitative analysis of the adaptive responses to 85 % oxygen in the rat lung and heart. Biochim Biophys Acta 1523(2–3):209–216

Ferraro SA, Yakisich JS, Gallo FT, Tasat DR (2011) Simvastatin pretreatment prevents ambient particle-induced lung injury in mice. Inhal Toxicol 23(14):889–896

Ferraro SA, Curutchet G, Tasat DR (2012) Bioaccessible heavy metals-sediment particles from Reconquista River induce lung inflammation in mice. Environ Toxicol Chem 31(9):2059–2068

Forastiere F, Stafoggia M, Picciotto S, Bellander T, D'Ippoliti D, Lanki T et al (2005) A case-crossover analysis of out-of-hospital coronary deaths and air pollution in Rome, Italy. Am J Respir Crit Care Med 172(12):1549–1555

Ghio AJ, Devlin RB (2001) Inflammatory lung injury after bronchial instillation of air pollution particles. Am J Respir Crit Care Med 164(4):704–708

Ghio AJ, Suliman HB, Carter JD, Abushamaa AM, Folz RJ (2002) Overexpression of extracellular superoxide dismutase decreases lung injury after exposure to oil fly ash. Am J Physiol Lung Cell Mol Physiol 283(1):L211–L218

GoogleMaps La Carcova, Buenos Aires Argentina. Images ©2012 Cnes/Spot Image, DigitalGlobe, TerraMetrics, data from map ©2012 Google, Inav/Geosystems SRL. Undetermined scale, "Google Maps." https://maps.google.com.ar/?ll=-34.522788,-58.581719&spn=0.020048,0.042272&t=k&z=15. Accessed 2 Dec 2013

Gurgueira SA, Lawrence J, Coull B, Murthy GG, Gonzalez-Flecha B (2002) Rapid increases in the steady-state concentration of reactive oxygen species in the lungs and heart after particulate air pollution inhalation. Environ Health Perspect 110(8):749–755

Henderson RF (2005) Use of bronchoalveolar lavage to detect respiratory tract toxicity of inhaled material. Exp Toxicol Pathol 57(Suppl 1):155–159

Krewski D, Snyder R, Beatty P, Granville G, Meek B, Sonawane B (2000) Assessing the health risks of benzene: a report on the benzene state-of-the-science workshop. J Toxicol Environ Health A 61(5–6):307–338

Leong BK, Coombs JK, Sabaitis CP, Rop DA, Aaron CS (1998) Quantitative morphometric analysis of pulmonary deposition of aerosol particles inhaled via intratracheal nebulization, intratracheal instillation or nose-only inhalation in rats. J Appl Toxicol 18(2):149–160

Li N, Venkatesan MI, Miguel A, Kaplan R, Gujuluva C, Alam J et al (2000) Induction of heme oxygenase-1 expression in macrophages by diesel exhaust particle chemicals and quinones via the antioxidant-responsive element. J Immunol 165(6):3393–3401

Lowry OH, Rosebrough NJ, Farr AL, Randall RJ (1951) Protein measurement with the Folin phenol reagent. J Biol Chem 193(1):265–275

Maehly AC, Chance B (1954) The assay of catalases and peroxidases. Methods Biochem Anal 1:357–424

Magnani ND, Marchini T, Tasat DR, Alvarez S, Evelson PA (2011) Lung oxidative metabolism after exposure to ambient particles. Biochem Biophys Res Commun 412(4):667–672

Mantecca P, Farina F, Moschini E, Gallinotti D, Gualtieri M, Rohr A et al (2010) Comparative acute lung inflammation induced by atmospheric PM and size-fractionated tire particles. Toxicol Lett 198(2):244–254

Marchini T, Magnani N, D'Annunzio V, Tasat D, Gelpi RJ, Alvarez S et al (2013) Impaired cardiac mitochondrial function and contractile reserve following an acute exposure to environmental particulate matter. Biochim Biophys Acta 1830(3):2545–2552

Miller MR, Shaw CA, Langrish JP (2012) From particles to patients: Oxidative stress and the cardiovascular effects of air pollution. Future Cardiol 8(4):577–602

Misra HP, Fridovich I (1972) The role of superoxide anion in the autoxidation of epinephrine and a simple assay for superoxide dismutase. J Biol Chem 247(10):3170–3175

Molinari BL, Tasat DR, Fernandez ML, Duran HA, Curiale J, Stoliar A et al (2000) Automated image analysis for monitoring oxidative burst in macrophages. Anal Quant Cytol Histol 22(5):423–427

Nel AE, Diaz-Sanchez D, Li N (2001) The role of particulate pollutants in pulmonary inflammation and asthma: Evidence for the involvement of organic chemicals and oxidative stress. Curr Opin Pulm Med 7(1):20–26

Nurkiewicz TR, Porter DW, Barger M, Millecchia L, Rao KM, Marvar PJ et al (2006) Systemic microvascular dysfunction and inflammation after pulmonary particulate matter exposure. Environ Health Perspect 114(3):412–419

Oberdorster G (2001) Pulmonary effects of inhaled ultrafine particles. Int Arch Occup Environ Health 74(1):1–8

Osornio-Vargas AR, Bonner JC, Alfaro-Moreno E, Martinez L, Garcia-Cuellar C, Ponce-de-Leon Rosales S et al (2003) Proinflammatory and cytotoxic effects of Mexico City air pollution particulate matter in vitro are dependent on particle size and composition. Environ Health Perspect 111(10):1289–1293

Perrone MG, Gualtieri M, Consonni V, Ferrero L, Sangiorgi G, Longhin E et al (2013) Particle size, chemical composition, seasons of the year and urban, rural or remote site origins as determinants of biological effects of particulate matter on pulmonary cells. Environ Pollut 176:215–227

Pope CA 3rd, Burnett RT, Krewski D, Jerrett M, Shi Y, Calle EE et al (2009) Cardiovascular mortality and exposure to airborne fine particulate matter and cigarette smoke: shape of the exposure–response relationship. Circulation 120(11):941–948

Ristovski ZD, Miljevic B, Surawski NC, Morawska L, Fong KM, Goh F et al (2012) Respiratory health effects of diesel particulate matter. Respirology 17(2):201–212

Rosas Perez I, Serrano J, Alfaro-Moreno E, Baumgardner D, Garcia-Cuellar C, Martin Del Campo JM et al (2007) Relations between PM10 composition and cell toxicity: A multivariate and graphical approach. Chemosphere 67(6):1218–1228

Saldiva PH (1998) Air pollution in urban areas: the role of automotive emissions as a public health problem. Int J Tuberc Lung Dis 2(11):868

Schins RP (2002) Mechanisms of genotoxicity of particles and fibers. Inhal Toxicol 14(1):57–78

Segal AW (1974) Nitroblue-tetrazolium tests. Lancet 2(7891):1248–1252

Singhal PC, Sharma P, Kapasi AA, Reddy K, Franki N, Gibbons N (1998) Morphine enhances macrophage apoptosis. J Immunol 160(4):1886–1893

Southam DS, Dolovich M, O'Byrne PM, Inman MD (2002) Distribution of intranasal instillations in mice: Effects of volume, time, body position, and anesthesia. Am J Physiol Lung Cell Mol Physiol 282(4):L833–L839

Tao F, Gonzalez-Flecha B, Kobzik L (2003) Reactive oxygen species in pulmonary inflammation by ambient particulates. Free Radic Biol Med 35(4):327–340

Tasat DR, de Rey BM (1987) Cytotoxic effect of uranium dioxide on rat alveolar macrophages. Environ Res 44(1):71–81

Torricelli AA, Novaes P, Matsuda M, Alves MR, Monteiro ML (2011) Ocular surface adverse effects of ambient levels of air pollution. Arq Bras Oftalmol 74(5):377–381